A Novel Approach for Hydraulic Valve Experimental Assessment Under Cavitating Condition

Domenico Mario Cavallo, Ornella Chiavola,
Edoardo Frattini and Fulvio Palmieri[*]

Università degli Studi Roma TRE, Dipartimento di Ingegneria Industriale Elettronica e Meccanica, Via Vito Volterra 62, 00146 Roma, Italy
E-mail: fulvio.palmieri@uniroma3.it
[*]*Corresponding Author*

Abstract

The article presents a novel approach for the experimental characterization of hydraulic valves. The proposed methodology allows to capture the key layout of the valve, to study its characteristic flow rate and to visualize the flow that passes through it. In the wake of the experimental technique found in the literature, the novel approach introduces the use of an original test valve, briefly called "prismatic". It represents an effective alternative to the so-called "Half-Cut Model" (HCM) proposed by Oshima and Ichikawa. The new test valve simplifies the experimental set-up and allows to visualize the whole internal flow field, providing full insight in both the inception and the spatial development of the cavitation. Moving from the HCM, the key features of the prismatic valve are preliminarily investigated and assessed by modelling, trough 3-D CFD simulations within OpenFOAM environment. Once the layout of prismatic valve is defined, the experimental assessment

phase is carried out, highlighting its capability in research and development activities.

1 Introduction

Valve performance affects the behavior of hydraulic systems significantly; the typical parameter used to characterize the flow through the valve restriction is the discharge coefficient. It is experimentally evaluated in the valve relevant operating range, and it allows to model the flow rate through the valve, under steady conditions [1–3].

Here, the attention is focused on poppet valves, widely used in the field of fluid power, and appreciated for their technical characteristics.

Although several articles in the literature cover various topics about poppet valves, it is useful to consider those contributions that tightly relate to the aim of the current effort. In [4–8], Oshima et al. take into consideration and analyze the flow conditions in which cavitation affects the conical poppet valves; among the considered topics, it is highlighted how cavitation causes significant flow alterations, leading to the "saturation" of the flow rate despite the increasing pressure drop across the valve.

The investigations reported in [4] are carried out using the "half-cut model", which consists of a prototype-valve which is cut in half along the symmetry axis, and which is provided with a transparent window for flow visualization.

It must be highlighted that the visualization of the flow plays a fundamental role in valve analysis, especially in those cases where critical conditions such as cavitation occur. The optical access to the internal flow of the valves is achieved through different techniques. Despite the variety of the approaches found in the literature, in any case the aim is to reach a satisfactory compromise between the possibility of observing the flow and the intrusiveness of the measurement; in some cases, transparent components in acrylic material are used, whether in cartridge type [9] or in the spool type valves [10]; in other cases, optical accesses are realized on the bodies of real valves [11]; some other contributions, such as [12], report investigations carried out on valve replicas or prototypes.

In this work, an alternative to the half-cut valve method [4] is proposed and assessed. It is based on the introduction of an equivalent test section to

replace the "half-cut model". The proposed approach, based on the "prismatic valve model", allows to simplify the construction of the test valve. It also allows to reduce the test flow rate and, at the same time, the flow field in the valve is fully visible (i.e., flow field is not hidden by the poppet) and diffused light backlighting technique can be adopted. Such approach represents an original adaptation of the Winklhofer experiment [13], well known in the field of high-pressure injection nozzles for internal combustion engines. The Winklhofer flow is realized across a simple layout step-channel, whose fundamental feature is to promote cavitation under full optical access, providing precious information for models' validation. The "prismatic model" here presented replaces the step-channel with the real valve profile, aiming at reproducing the hydraulic flow within a real-like test section. Moreover, the technique here proposed introduces the possibility of continuously adjusting the opening of the test section. This feature may not be crucial in the context of models' validation, but it is essential investigating hydraulic valves. The current article describes the details of the proposed method and reports the main results obtained from its assessment. After a preliminary investigation by modeling, the equivalent test-section is experimentally characterized under steady pressure conditions. This activity is associated to the flow visualization, with the aim to identify the cavitation inception, its development, and its spatial distribution within the valve.

2 Materials and Method

2.1 Experimental Hydraulic System

Upstream the test section, pressure is maintained at constant level, avoiding fluctuations. These conditions are achieved through the closed-loop control of pressure in delivery ambient, by the variable speed of an external gear pump. With reference to Figure 1, the transducer (PT1) reads the actual pressure of delivery ambient (DA) and the controller points the desired pressure by regulating the speed (W) of the pump shaft (P).

Throttle (TH1) sets the test back-pressure, ranging from the upstream to the atmospheric pressure. Flow rate through the valve is measured by (FM1). A hydro-pneumatic accumulator (HA) eliminates pressure fluctuations upstream the test valve; the piezo-resistive transducer (PR) is used to check the extent of the residual pressure fluctuation in any operating condition. An alarm signal is sent to the operator if the pressure fluctuation exceeds 1% of the average value over a period of pump rotation. Table 1 presents the characteristics of the main hydraulic instrumentation.
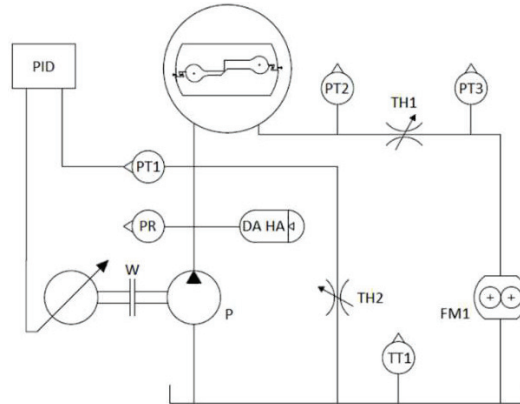
Figure 1   Sketch of the hydraulic system.

Table 1   Hydraulic instrumentation

	Type	Range	Linearity	Repeatability
FM1	External gear	0.05–80 l/min	±0.3%	±0.05%
			of measured value	
			Linearity	Hysteresis
PR	Piezo-resistive	0–50 bar	±0.2% FSO	0.2% FSO
				Accuracy
PT (#)	Strain gauge	0–50 bar		±0.1% FSO
TT1	RTD	273.15–373.15K		±0.1% FSO

Table 2   Hydraulic fluid properties

	Method	Unit	
Density @ 288.15K	ASTM D 4052	kg/m^3	886
Viscosity @ 313.15K	ASTM D 445	mm^2/s	68
Viscosity Index	ASTM D 2270	–	97
Flash point	ASTM D 92	K	508.15
Pour point	ASTM D 97	K	249.15

The test rig is equipped with a thermoregulation system, which allows the closed-loop temperature control of the working fluid. In the experiments, the commercial hydraulic fluid Tellus S2 M 68 by Shell is used. Table 2 reports its main specifications.

The experimental hydraulic system is used under a test protocol that is preliminarily defined. As a first step, the hydraulic fluid and the system components are thermoregulated until the thermal steady condition is reached.

Then, the investigations are repeated several times, by following a random sequence of operating conditions of the test valve. Each test condition is easily obtained by regulating the opening of TH1 valve.

2.2 The Equivalent Test-section

The "prismatic model" of the poppet valve is part of a multi-layer assembly; Figure 2 shows an exploded view of the prototype valve. A support element (a) houses the inlet (X1) and the discharge (X2) connections to the hydraulic test system.

The transparent element (b) is made of methyl methacrylate and is provided with passages for the fluid, (b1) and (b2), centered on the axis of the hydraulic connections on (a). Methyl methacrylate is compatible with the experimental set up. It meets the required structural specifications, and it
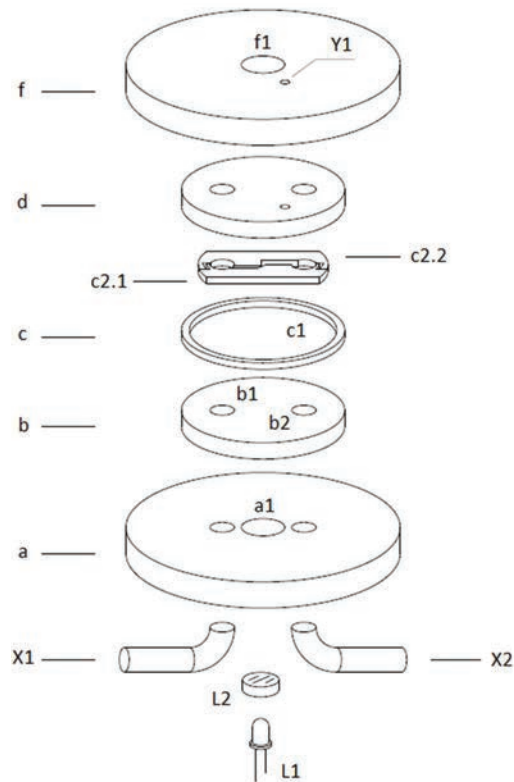
Figure 2 "Equivalent test section", exploded view.

Table 3	Equivalent test-section components
L1	Light Emission Diode (4×4 SMD)
L2	Light diffuser
X1, X2	Inlet and outlet connections
a, f	Steel metal plates
a1, f1	Observation hole
d, b	Methyl methacrylate elements
b1, b2	Hydraulic passages
c, c2.1, c2.2	Prismatic model
c1	Sealing ring
Y1	Hydraulic outlet for sealing ring
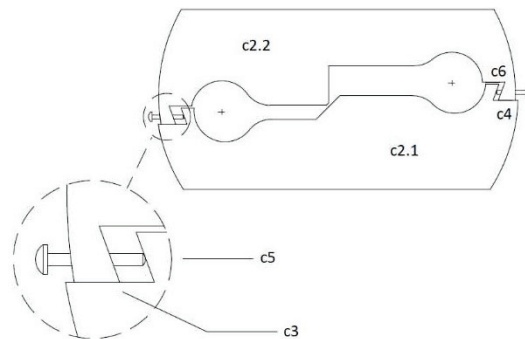
Figure 3   Prismatic model.

withstands the stresses induced by the cavitating flow. It ensures the absence of leakages, without gaskets or other sealing media. At chemical level, it is compatible with the hydraulic fluids. Furthermore, it is easily available, at very low cost, on the market. Table 3 reports the list of the main component of the test-section.

Element (c) constitutes the "prismatic model" of the poppet valve. It is made of three parts; (c1) is a sealing ring that surrounds the elements (c2.1) and (c2.2). The internal ambient sealed by the ring is placed at low pressure through the hydraulic outlet (Y1), which reports any fluid leaks to the atmospheric tank.

Both the ring (c1) and the element (c2.2) are equipped with positioning pins that block their position on the transparent element (b), facilitating assembly and set-up operations.

The transparent methacrylate element (d) realizes the second optical access to the valve, in combination with plate (f) and its observation hole

(f1). The observation hole (a1) houses the lighting device (L1) and the diffuser (L2).

The elements (c2.1) and (c2.2) together form the prismatic model and reproduce the profile of the poppet valve, as shown in Figure 3. They are mechanically coupled through the conjugate surfaces (c3 and c4) and the adjustable stops (c5 and c6).

The parallelism of the shared surfaces c3 and c4 is achieved with high accuracy, and it is guaranteed through a grinding process under close dimensional tolerance (below 1 μm). Through the same machining process, the edges of the oil passage and the two sides of the metering restriction of are produced, ensuring parallelism and surface finish as usual in hydraulic poppet valves. Every edge of the metering restriction profile is sharp.

The conjugate surfaces create the hydraulic seal that separates the high-pressure zone from the ambient pressure zone; the adjustable stops allow effective positioning of one element with respect to the other, i.e., the position of the poppet with respect to the seat.

The optical access allows the visualization of the cavitating areas using the diffused light backlighting technique. The lighting device (symbolized in Figure 4 with L1) consists of an array of high brightness LEDs with a PWM driver. The diffuser element (L2) is made using a high-density flat lens. The images are captured by a high-resolution C-MOS (K) digital camera installed on a microscope (Z). Table 4 reports the key-features of visualization system.
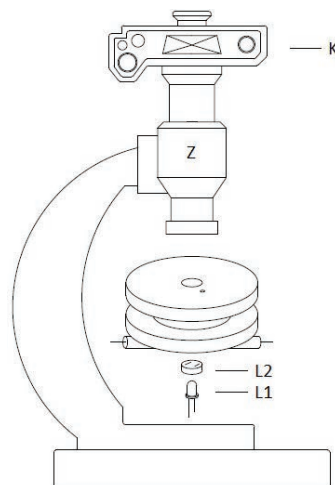

Figure 4   Schematic of flow visualization system.

Table 4   Visualization system

C-MOS sensor	24×36 mm – 36 MPixel
C-MOS sensitivity	100 to 25600 ISO
Camera shutter time	Open shutter during strobe light time
Optics	Carl Zeiss STEMI 508
Strobe light type	Light Emission Diode (4×4 SMD)
Strobe light-time	Adjustable in the range 100 μs to 1 s
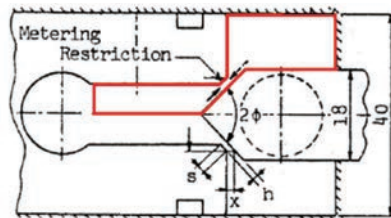
s = 1.32 mm   2Φ = 90 degrees   x and h depend on poppet lift

Figure 5   Valve profile extraction (elaborated from [5]).
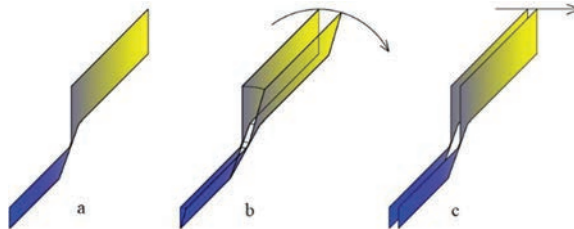
**Figure 6**   a, Valve profile; b, "thin cylindrical" layout; c, "prismatic" layout.

The considered valve profile replicates the layout of the "half-cut model" (Figure 5) reported in [5]. It is thus useful to compare two "thin" geometries, the one cylindrical, the other prismatic as shown in Figure 6; the "thin cylindrical" is derived from a sector of the real geometry. Neglecting boundary effects, the flow through this geometry is the same as that observed in the real valve.

Considering the alternative geometry, here defined as "prismatic", the parallelism of the boundary faces alters the original passage sections. In fact, throat section, poppet lift and valve profile being the same, in the prismatic layout the upstream sections are increased while the downstream sections are reduced. It should now be noted that the real valves are designed so that the throttling area is not significantly affected by the upstream and downstream
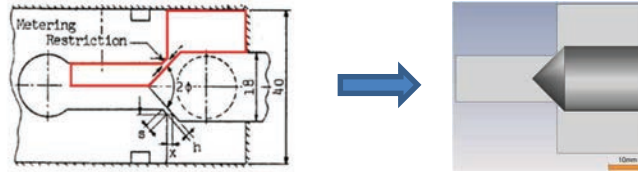
Figure 7 Transition from HCM layout to computational domain.
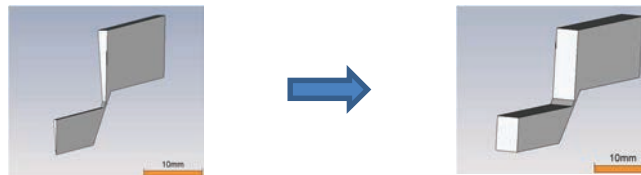
Figure 8 From cylindrical to "prismatic model".

sections; in the case under examination, the alterations introduced in the upstream and downstream sections are still negligible when compared to the valve throttling section, even at full poppet lift.

The layout of the prismatic valve is defined in the light of a preliminary investigation based on 3D-CFD modelling; transition from cylindrical to prismatic geometry, boundary effects and the presence of the supply and discharge hydraulic connections are considered and assessed.

2.3 Assessment of Prismatic Layout by Modeling

2.3.1 Computational domain of hydraulic test-section

According to the valve layout found in [4], the flow domain is extracted to generate the computational grids (Figure 7).

The computational grid, due to the cylindrical symmetry of the valve, is conveniently limited to a sector of the flow domain. Moving from such a cylindrical layout, the "prismatic model" is built; it is obtained by "extrusion" of the valve section, as shown in Figure 8.

2.3.2 CFD modeling

2.3.2.1 *Multiphase flow modeling*

The simulation campaigns are carried out in OpenFOAM environment [14], where a RANS approach with *k-OmegaSST* closure is adopted [15]. The modeling of cavitating turbulent flow is based on the Homogeneous Equilibrium Model (HEM). It assumes the perfect mixing of liquid and vapor phases and

Table 5   Computational meshes

	Min Cell Number	Max Cell Number	Adopted
Cylindrical model	8000	256000	50000
Prismatic model	16000	512000	200000

at each computational cell the set of conservation equations are solved for the mixed phase [16]. The adopted cavitation model is CavitatingFoam [17].

2.3.2.2 *Computational meshes*

Structured meshes made of hexahedral elements are used, both for the simulation of prismatic geometry and for cylindrical geometry. A preliminary test phase is devoted to find the proper configuration in terms of mesh refinement; by progressively increasing the cell density in the simulated problems, the correct mesh resolution is established evaluating, beside the 3-D flow pattern features, the mass flow rate predictions among the computational cases. The structured meshes of prismatic model is created within SALOME 9.4.0 environment [18], whereas the cylindrical model is meshed within OpenFOAM environment. Since the cross section of the cylindrical valve model is a liquid surface, slip boundary conditions are used. Given that the boundaries of the prismatic valve model are a material surface, the viscous effects are modeled, and the standard wall function approach is adopted [15].

The features of the adopted computational grids are reported in Table 5. The properties of the cylindrical and prismatic meshes at the same poppet lift (x = 0.840 mm) are reported in Table 6.

2.3.3 CFD investigation

As a first step, the consistency of prismatic model in respect to the model of standard cylindrical layout derived by Oshima [4] is assessed; then, the boundary effects induced by the transparent windows are discussed and the thickness of the research-valve is determined. Finally, the influence of the hydraulic connections of the research-valve is considered. According to Oshima experiments [5], simulations are carried out maintaining 50 bar constant pressure at valve inlet section. Seven values of pressure drop are tested across the throttle, 10 bar, 20 bar, 25 bar, 30 bar, 35 bar, 40 bar and 50 bar. Different poppet lifts in the range 0,3–0,9 mm are simulated. The inception and development of cavitation, and more in general, the similar flow features of cylindrical and prismatic layouts result in the hydraulic behavior (flow rate vs. pressure difference) in all simulated cases.

Table 6 Mesh properties

	Max Aspect Ratio	Average Non-orthogonality	Max Skewness
Cylindrical layout	97	11.5	0.6

	Max Aspect Ratio	Average Non-orthogonality	Max Skewness
Prismatic layout	93	7.54	0.56

Figure 9 – *Up* shoes, for each layout, the average throat velocity, and the discharge coefficient at 0.840 mm lift. The average throat velocity is computed as the average flow velocity normal to the throat cross section. Comparing the trends, very close hydraulic behaviors are highlighted, and flow rate saturation starts at the same pressure drop (35 bar).

The down chart of Figure 9 reports the results related to other configurations of the prismatic model, depending on its thickness. In the simulations, thickness ranges from 1 to 6 mm. The results indicate that above 3 mm, flow rate it is not affected by thickness; thus, 4 mm is chosen as a reliable thickness for the research-valve set-up.

Close agreement among the flow patterns is shown comparing scalar velocity and pressure maps, in all the tested cases. Even at beginning of hydraulic saturation, when flow conditions are critical, very similar behavior characterizes flow field. Figure 10 shows inception of cavitation in terms of vapor/liquid fraction time-averaged maps, for cylindrical and prismatic layouts.

Once the hydraulic behavior of the prismatic model is assessed, the investigations are moved to the last step, since inlet and outlet ports must be provided in the actual implementation of the prismatic model, as shown in Figure 11.
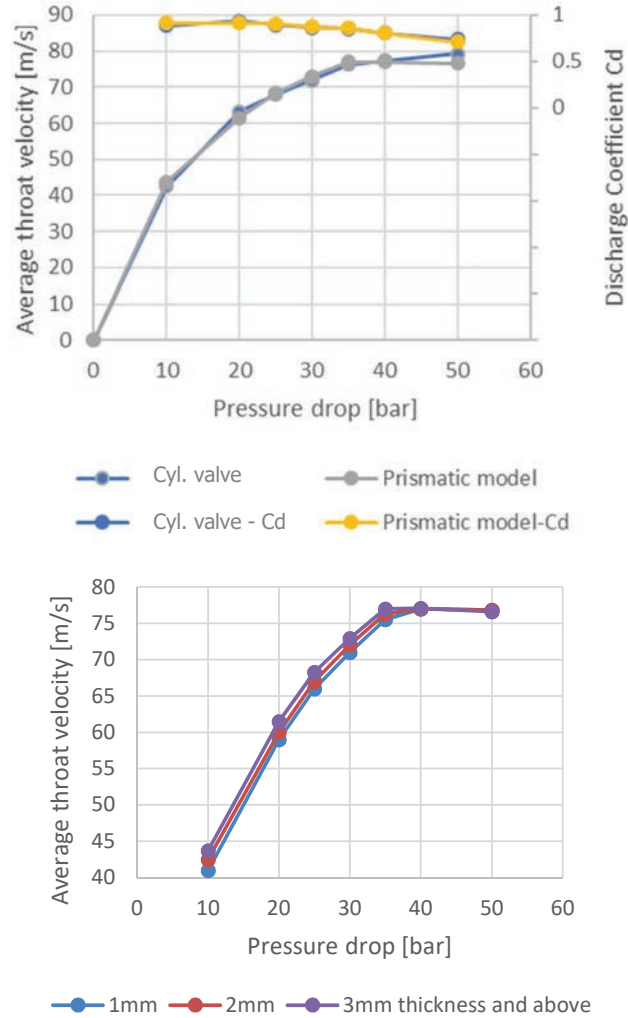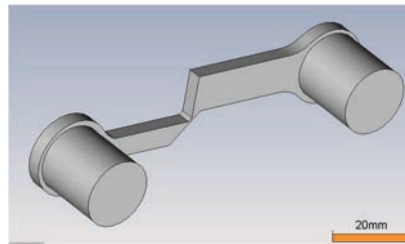
Figure 9 *Up* – Average throat velocity and discharge coefficient vs. pressure difference of Prismatic Valve and Circular Sector Valve; x = 0.840 mm poppet lift; *Down* – Effect of model thickness (prismatic valve).

The trends reported in Figure 12 allow to compare the simple prismatic layout with the actual implemented layout, in terms of average throat velocity and discharge coefficients; close agreement is found, in all the tested cases. Thus, the prototype of the equivalent test-section is built as described in paragraph 0. Figure 13 reports a view of the valve under set-up.
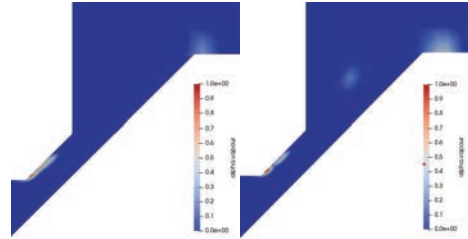
Figure 10 Cavitation inception (*Left*: cylindrical layout; *Right*: prismatic layout); poppet lift = 0.565 mm; pressure drop = 35 bar.


**Figure 11** Actual fluid domain of prismatic valve setup.
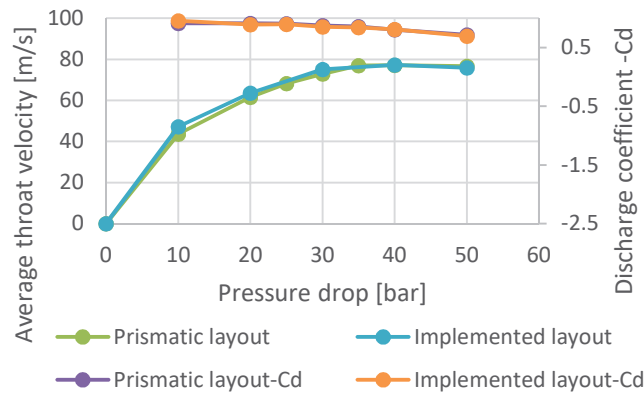
Figure 12 Average throat velocity and discharge coefficient vs. pressure drop for actual and prismatic valve; poppet lift = 0.840 mm.

3 Results

The results are organized in the attempt to effectively highlight the behavior of the prismatic model at hydraulic test rig. The first group of results reports the hydraulic behavior of the valve as the pressure drop varies, poppet lift
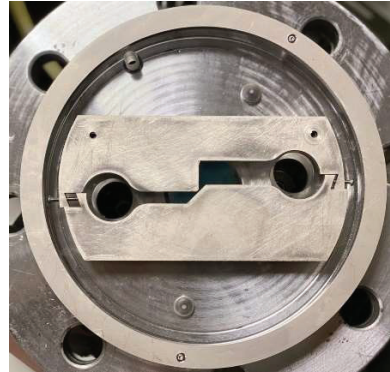
Figure 13   Partially assembled equivalent test-section.
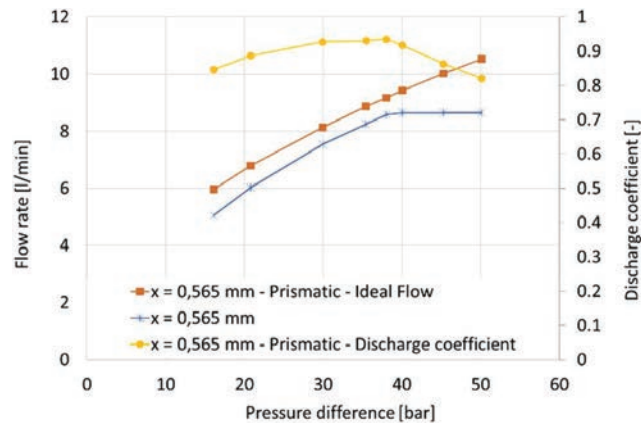
Figure 14   Flow rate and discharge coefficient vs. pressure difference; x = 0.565 mm poppet lift.

being the same. Under six reference pressure conditions (stages 1 to 6), the internal flow features of the valve are reported and discussed. Hence, two other groups of results are presented, exploring the "low" and the "high" openings of the poppet. In a further step, the link between the poppet opening and the discharged flow is discussed, in the light of the reference-results available in the literature.
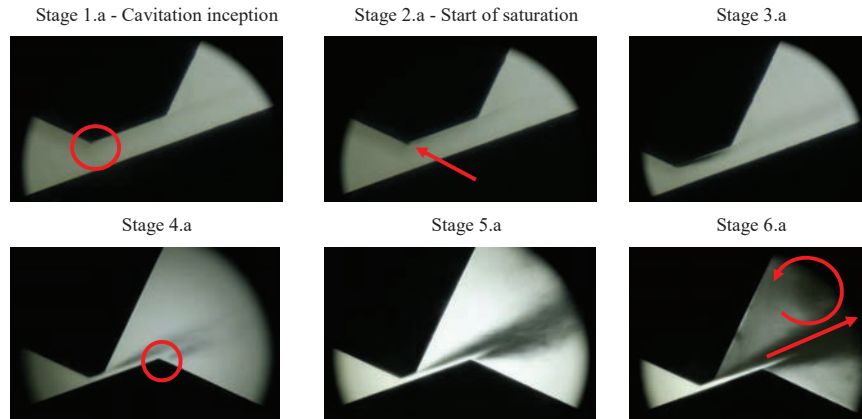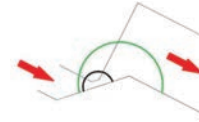
3.1 Intermediate Poppet Lift

Figure 14 reports the trends of flow rate and flow coefficient versus the pressure difference across the valve; upstream pressure is kept constant at

Table 7 Flow visualization referred to the six stages of Figure 14

x = 0.565 mm – Prismatic – Experimental

Fields of view on the valve – Wide view, green – Detail view, black

Stage 1.a - Cavitation inception	Stage 2.a - Start of saturation	Stage 3.a

| Stage 4.a	Stage 5.a	Stage 6.a

50 bar. The graphs refer to 0.565 mm poppet lift. The flow rate curve has a regular behavior up to a certain value of the pressure difference, after which saturation occurs. In such operating field, flow rate ceases to increase, despite the increase in pressure drop; this behavior is linked to the reduction of the effective passage section due to cavitation development. The trend of the flow coefficient allows to effectively highlight the role of cavitation on the flow through the pilot section of the valve. Alongside the trends of Figure 14, further insight is made possible by the flow visualization (Table 7). The images in the table refer to the pressure conditions indicated with a black mark in Figure 14, numbered from 1 to 6. The optical investigation allows the research of cavitation inception condition, whose occurrence is in advance of flow saturation. The point where cavitation appears is the inlet edge of the seat chamfer, as highlighted by the red circle on stage 1.a.; here, the extent of cavitating flow region is small when compared to the throat section, so that the effect on discharge coefficient is still limited. The presence of cavitation is also associated with emission of a typical noise, clearly distinguishable by ear despite the presence of ambient noise (e.g. gear pump, electric drive). However, in the inception phase (stages 1.a and 1.b) noise emission is relatively weak and specific acoustic measurements are needed.

The extent of cavitating regions is investigated through the flow visualization as the downstream pressure changes. Since cavitation is a typical unsteady phenomenon, the extent of cavitating regions varies aleatorily in time. Thus, the exposure time for image acquisition is chosen long enough to catch the full wake of cavitating regions. In the initial stages of saturation (stages 2.a and 3.a), the cavitation region extends downstream of the inception point, reaching a large part of the seat chamfer length. In the more advanced stages, a second inception point is present at poppet edge (stage 4.a). The lower is the downstream pressure, the stronger is the character of cavitation (stage 5.a), until intense flow recirculation is observed (stage 6.a).

3.2 Low Poppet Lift

By reducing the valve opening, the change in the flowrate/pressure trend is evident. According to Figure 15, the saturation start needs higher pressure difference than previous case. Due to the seat chamfer, low lift conditions guide the flow in a sort of channel. The development of cavitation reflects this condition; on the one hand, the cavitating region tends to spread closer to the center line of the channel, as suggested by the stages 3.b and 4.b (Table 8), when compared to the corresponding ones in Table 7. On the other hand, the flow tends to detach more brutally downstream the throat; this means that in stage 5.b, there is still a cavitating region of modest extension attached to the second edge of the chamfer, while in stage 6.b cavitation fills the volume downstream the second edge of the chamfer.
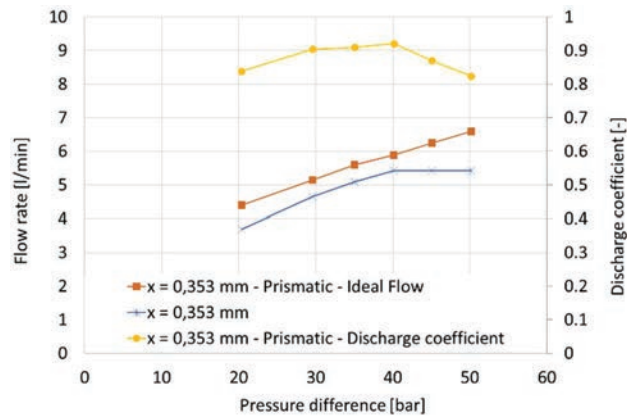
Figure 15   Flow rate and discharge coefficient vs. pressure difference; x = 0.353 mm poppet lift.

Table 8   Flow visualization referred to the six stages of Figure 15

x = 0.353 mm – Prismatic – Experimental

Stage 1.b	Stage 2.b	Stage 3.b

Stage 4.b	Stage 5.b	Stage 6.b
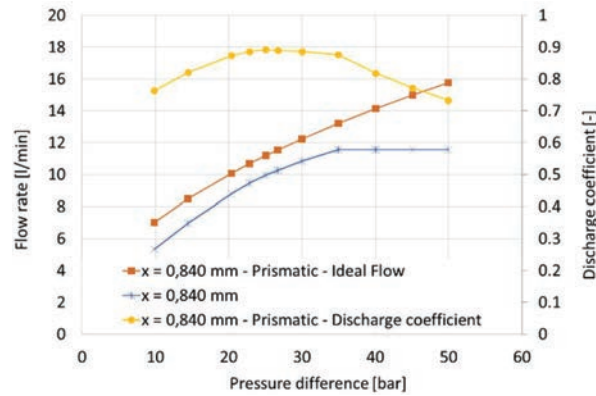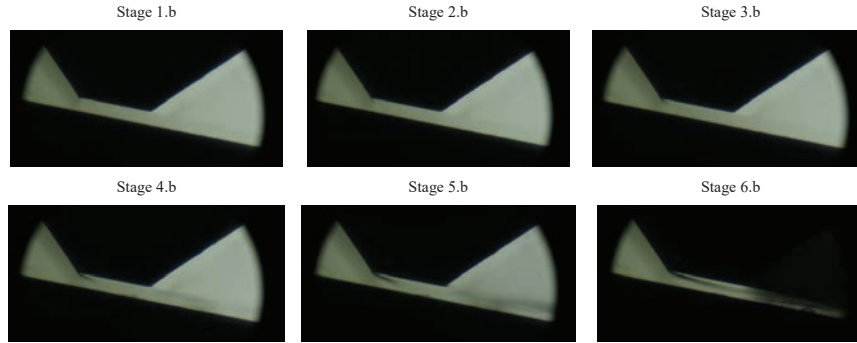
**Figure 16**   Flow rate and discharge coefficient vs. pressure difference; x = 0.840 mm poppet lift.

3.3 High Poppet Lift

Figure 16 shows the trends relating to the maximum poppet lift (x = 0.840 mm). Cavitation inception point and start of saturation are in advance when compared to the base case (x = 0.565 mm). The flow visualization reported in Table 9 reveals that cavitation behavior resembles the features of base case; indeed, the extent of cavitation regions downstream of the chamfer edge do not reach the level of the low-lift case.

3.4 Novel Approach Assessment

Beside the consistency found at modeling level (paragraph 2.3), the experimental behavior of the prismatic test section is in full agreement with what

Table 9 Flow visualization referred to the 6 stages of Figure 16
x = 0.840 mm – Prismatic – Experimental

Stage 1.c   Stage 2.c   Stage 3.c

Stage 4.c   Stage 5.c   Stage 6.c
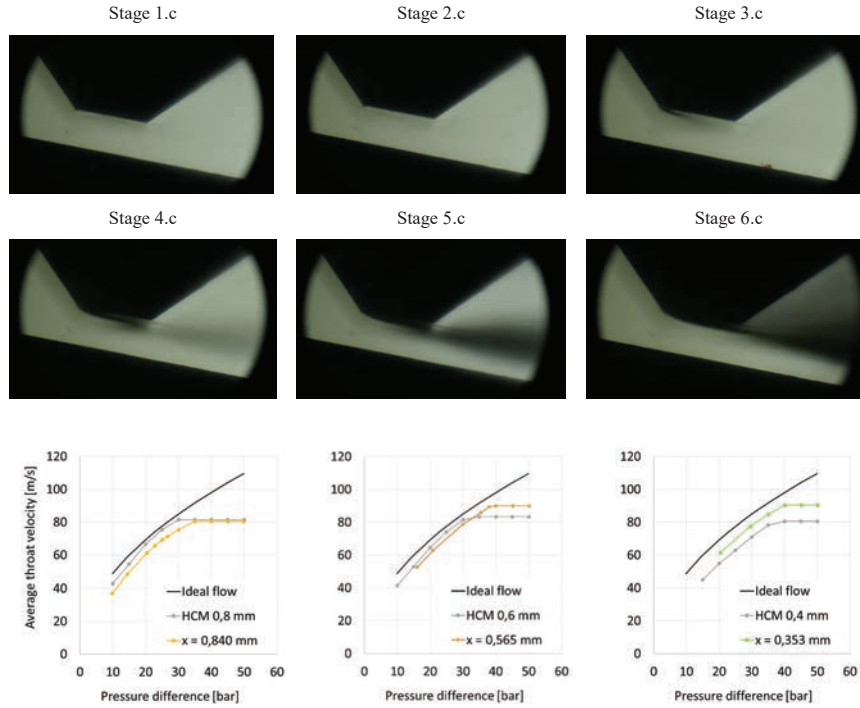
Figure 17 Average flow velocity at throat section vs. pressure difference: comparison between "Prismatic model" and "Half Cut Model – HCM" (elaborated from [5]).

obtained by Oshima [5] on the half-cut model. In fact, the experiments conducted by Oshima have revealed that the beginning of the saturation zone shifts to the left as the valve opening increases, and that cavitation inception happens before (in terms of pressure difference) the start of saturation. A direct comparison at experimental level with the results of Oshima is at least unproper, since the characteristics of the original experiment set up are not known (surface finishes, characteristics of materials, manufacturing tolerances, hydraulic fluid properties and contamination). However, the measured flow rates and the geometrical throat sections of both prismatic valve and half-cut model [5] give the chance to compare the flow velocity at throat section. As reported in Figure 17, the agreement is well consistent in the same opening range of the poppet and in the same pressure conditions tested by Oshima.

4 Conclusion

The article presents and assesses a new investigation approach for the analysis of hydraulic valves. The proposed approach introduces the "prismatic" model, a research-valve that supports the experiments: its construction is evidently plain, and the range of test flowrates is reduced in comparison to the standard approach, valve geometry being the same.

3-D CFD simulation campaigns within OpenFOAM environment highlight the approach reliability and lead its implementation at experimental level, providing full information for the set-up of the research-valve at test rig (valve thickness and inlet-outlet hydraulic connections).

The experimental investigations allow to determine the steady characteristics of the test-valve for three different poppet lift levels, providing the trends of the discharge coefficients. The behavior of the proposed prismatic valve results in full agreement with the reference-contributions found in the literature, confirming the validity of the approach.

Beside its capability to catch the hydraulic behavior of the poppet valves, the new approach allows the visualization of the whole flow field. Such a feature is fundamental to provide a deep insight on both inception and behavior of cavitation. Evidently, such information constitutes the basis for the design phases of similar valves, as well as for the validation or development phases of three-dimensional cavitation models in the field of fluid power.

References

[1] R. Von Mises, 'Berechnung von Ausfluss – und Überfallzahlen', Zeitschrift des Vereins Deutscher Ingenieure, 1917.

[2] H. Murrenhoff, 'Grundlagen der Fluidtechnik – Teil1: Hydraulik', Umdruck zur Vorlesung, 8. Aufl. Herzogenrath: Shaker (Reihe Fluidtechnik U3), 2016.

[3] C. von Grabe, C. Riedel, C. Stammen, H. Murrenhoff, 'An Analytic Thermodynamic Model for Hydraulic Resistances Based on CFD Flow Parameters', International Journal of Fluid Power, 14(2), pp. 17–26, DOI: 10.1080/14399776.2013.10781072, 2013.

[4] S. Oshima, T. Ichikawa, 'Cavitation Phenomena and Performance of Oil Hydraulic Poppet Valve, 1st report, Mechanism of Generation of Cavitation and Flow Performance', Bull. Jap. Soc. Mech. Eng., 28(244), pp. 2264–2271, https://doi.org/10.1299/jsme1958.28.2264, 1985.

[5] S. Oshima, T. Ichikawa, 'Cavitation Phenomena and Performance of Oil Hydraulic Poppet Valve – 2nd report, Influence of The Chamfer Length of the Seat and the Flow Performance', Bull. Jap. Soc. Mech. Eng., 28(244) pp. 2272-2279, https://doi.org/10.1299/jsme1958.28.2272, 1985.

[6] S. Oshima, T. Ichikawa, 'Cavitation Phenomena and Performance of Oil Hydraulic Poppet Valve – 3rd report, Influence of the Poppet angle and Oil Temperature on the flow performance', Bull. Jap. Soc. Mech. Eng., 29(249), pp. 743–750, https://doi.org/10.1299/jsme1958.29.743, 1986.

[7] S. Oshima, T. Ichikawa, 'Cavitation Phenomena and Performance of Oil Hydraulic Poppet Valve – 4th report, Influence of Cavitation on the Thrust Force Characteristics', Bull. Jap. Soc. Mech. Engrs, 51(467), pp. 2249–2257, https://doi.org/10.1299/kikaib.51.2249, 1985.

[8] S. Oshima, T. Ichikawa, 'Cavitation Phenomena and Performance of Oil Hydraulic Poppet Valve – 5th report, Influence of Dimensions of Valve on the Thrust Force Characteristics', Bull. Jap. Soc. Mech. Engrs, 51(469), pp. 3023–3031 https://doi.org/10.1299/kikaib.51.3023, 1985.

[9] K. Kumagai, S. Ryu, M. Ota, K. Maeno, 'Investigation of Poppet Valve Vibration with Cavitation', International Journal of Fluid Power, 17(1), pp. 15–24, DOI: 10.1080/14399776.2015.1115648, 2016.

[10] H. Okabe, Y. Tanaka, A. Watanabe, F. Yoshida, S. Iio, Y. Haneda, 'Cavitation in a Spool Valve for Water Hydraulics', IOP Conference Series: Earth and Environmental Science, 240(6), art. no. 062029, DOI: 10.1088/1755-1315/240/6/062029, 2019.

[11] J. Zou, X. Fu, X. W. Du, X. D. Ruan, H. Ji, S. Ryu, M. Ochiai, 'Cavitation in a Non-Circular Opening Spool Valve with U-grooves', Proc. of the Instit. of Mech. Engineers, Part A: Journal of Power and Energy, 222(4), pp. 413–420, 2008. https://doi.org/10.1243/09576509JPE489, 2008.

[12] S. Washio, S. Kikui, S. Takahashi, 'Nucleation and Subsequent Cavitation in a Hydraulic Oil Poppet Valve', Proc. of the Instit. of Mech. Engineers, Part C: Journal of Mechanical Engineering Science 224(4), pp. 947-958, https://doi.org/10.1243/09544062JMES1618, 2010.

[13] E. Winklhofer, E. Kull, E. Kelz, A. Morozov, 'Comprehensive Hydraulic and Flow Field Documentation in Model Throttle Experiments under Cavitation Conditions', In Proc. of the ILASS-Europe Conference, DOI: 10.13140/2.1.1716.4161, Zurich, 2001.

[14] H. G. Weller, G. Tabor, H. Jasak, C. Fureby, "A Tensorial Approach to Computational Continuum Mechanics Using Object-Oriented Techniques", Computers in Physics, 12, 6, 1998.

[15] F. R. Menter, 'Improved Two-Equation k-omega Turbulence Models for Aerodynamic Flows', NASA TM 103975, October 1992.

[16] C. E. Brennen, 'Fundamentals of Multiphase Flow', Cambridge University Press, 2005. doi:10.1017/CBO9780511807169.

[17] F. P. Kärrholm, H. Weller, N. Nordin, 'Modelling Injector Flow Including Cavitation Effects for Diesel Applications', ASME 5th Joint Fluids Engineering Conference, FEDSM2007-37518, pp. 465-474; DOI 10.1 115/FEDSM2007-37518, San Diego CA, 2007.

[18] Open CASCADE, 'SALOME: The Open Source Integration Platform for Numerical Simulation', http://www.salome-platform.org.

Biographies

Domenico Mario Cavallo received the master's degree in mechanical engineering from Roma TRE University in 2018. He is currently a Ph.D. student in mechanical and industrial engineering at Roma TRE University. His research interests are in modelling, simulation and performance of the exhaust after treatment systems.
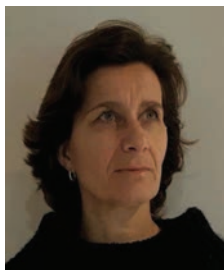
Ornella Chiavola received the master's degree in mechanical engineering from La Sapienza University in 1994 and the philosophy of doctorate degree

in Mechanical Engineering from Roma TRE University in 1999. She is currently working as Full Professor at the Department of Industrial, Electronical and Mechanical Engineering, Roma TRE University. Her research areas include internal combustion engines, environmental impacts of power plants, renewable energy systems and fluid machinery, fluid power components and systems.

Edoardo Frattini received the master's degree in 2019 from Roma TRE University. He is currently a Ph.D. student at the Department of Industrial, Electronical and Mechanical Engineering, Roma TRE University. His research areas include fluid power components and systems and internal combustion engines.

Fulvio Palmieri received the master's degree (2004) and the philosophy of doctorate degree (2009) in mechanical engineering from Roma TRE University. He is currently working as associate professor at the Department of Industrial, Electronical and Mechanical Engineering, Roma TRE University. His research areas include fluid power components and systems, internal combustion engines, renewable energy systems and fluid machinery.